MICRO PARTICLE INCLUSION IN A WATER LADLE MODEL WITH FOAMY OIL

Basheeruddin Faizaan Syed, Yun Liu, Xipeng Guo, Chenn Zhou

Purdue University Northwest
Address: 169th Street Hammond, IN 46323

Keywords: Steel Refining, Gas Stirred Ladle, Slag Entrainment, Micro Inclusion

ABSTRACT

Ladle metallurgy is a crucial secondary steelmaking process where micro-scale slag inclusions can form, compromising steel quality, especially during inert gas stirring. In this study, a scaled water ladle model, consisting of foamy sunflower seed oil and distilled water, is implemented to simulate the behavior of porous slag and molten steel. Compressed air, regulated with a high-precision flow rate meter, is injected into the model to replicate the gas- stirring process in ladle metallurgy. To observe the inclusion formation and generation at micro-scale, a high-speed camera system with four cameras is implemented to image four different sections of the water ladle model for achieving a high-resolution imaging and micro-scale inclusion count quantification.

INTRODUCTION

Secondary metallurgy, also known as the ladle metallurgy process, is essential for refining molten steel to improve its purity and mechanical properties [1]. During this process, gas stirring is a common practice that involves injecting inert gases, usually argon, into molten steel to generate turbulence, promoting homogenous mixing and facilitating the removal of inclusions (foreign particles) through slag-inclusion interactions. Inclusion, varying in size, held a considerable influence on the quality, durability, and performance of the steel product [2]. Due to low density and buoyancy, large inclusions tend to rise to the slag layer where they are absorbed and easily removed [3]. Micro-inclusions, however, are much smaller and less buoyant, making them difficult to rise. Consequently, they often remain suspended and dispersed throughout the molten steel, leading to steel product defects and impurity. Therefore, there is a great need for more intricate methods of inclusion control and reduction [4].

Costa e Silva provides an in-depth analysis on the classifications and origin of non-metallic inclusions (NMI) in steel and discusses various strategies for their control to finally improve the steel quality [5]. Miki and Thomas reported alumina inclusion from measuring a steel sample of 150 gram at 0.5 meters from the top of a 160-ton ladle. Inclusions were extracted using an acid technique to dissolve away the steel around the inclusion and inclusion size distributions were measured by a laser diffraction scattering method, revealing a typical alumina inclusion cluster size of only 4 microns. Meanwhile, a CFD simulation is carried out in a tundish model, suggesting a clear trend of strong inclusion removal for larger alumina clusters but less for smaller alumina clusters[6]. Akbari *et al* developed a 3D multiphase CFD with Population Balance Model to investigate the effect of gas purging positions on an industrial ladle's performance, including mixing time and inclusion removal with velocity, turbulence, shear stress and mass/heat transfer data. The result suggests that increased gas injection angle could improve ladle performance on inclusion removal and shear stress[7]. Using Automated Feature Analysis (AFA), Pitts-Baggett studied the slag emulsification on the samples collected during the Ladle Metallurgy Furnace (LMF) process. Micro-scale slag emulsification and slag

droplets, ranging from 30 to 200 microns, were observed and investigated, revealing an inversed correlation between desulfurization rate and slag droplet index[1]. Although CFD simulations have already revealed some interesting results on inclusion generation and removal, the Population Balance Model implemented in the simulation is primarily relying on theoretical inclusion source term estimation which is subject to significant error and uncertainty[8]. On the other hand, the physical water ladle modeling has been implemented to study macro-scale slag emulsifications without considering micro-scale inclusion. Therefore, a thorough understanding of the behavior of micro inclusions in a physical water ladle model is lacking and desired. In this study, we implemented a high-resolution imaging system on a gas stirred water ladle model for investigating the micro-inclusion behavior and inclusion count quantification.

EXPERIMENTAL PROCEDURE

To investigate the formation of inclusions and flow-induced slag entrainment at the water-oil interface, based on an industrial ladle, a 1/10 scaled physical model (40 cm x 25 cm x 2 cm) was developed with a small thickness for imaging and micro-inclusion quantification. To achieve high spatial resolution (95 μm/pixel) and facilitate detailed observations, the tank was divided into four equal quadrants, each measuring 15.5 cm × 12.5 cm. This configuration enables comprehensive tracking of particle and interface disturbances.

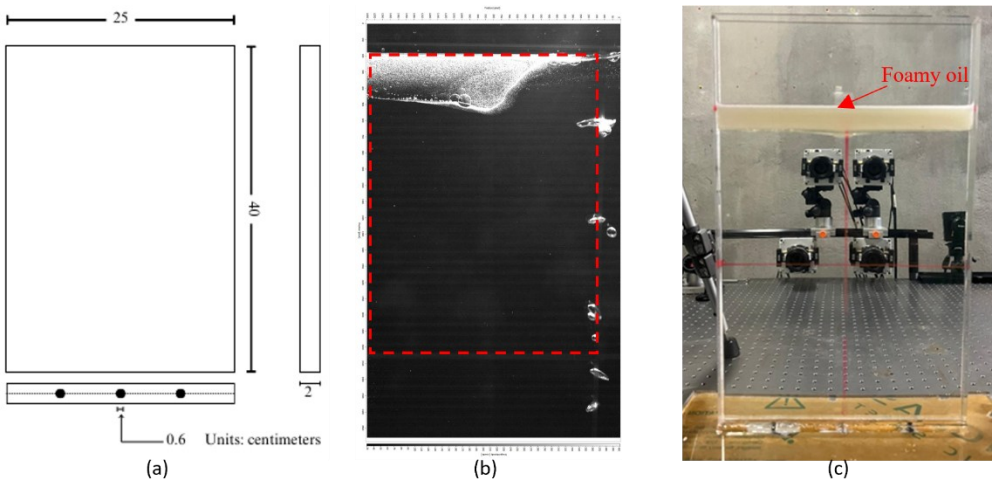

Figure 1: (a) Dimensions of water ladle tank (b) resizing for area of interest (c) Tank filled with distilled water and foamy oil

Four Phantom VEO 640 cameras, each monitoring a separate quadrant, were used to ensure complete visualization of slag entrainment and inclusion formation. These cameras were equipped with 50 mm Tokina macro lens (f/8) and operated at resolution of 2560 × 1600 pixels with a frame rate of 500 fps, ensuring high quality data acquisition. To ensure that only the relevant portion was analyzed, the images were cropped to focus on the area of interest. Due to this cropping, the ratio of the physical quadrant size to the pixel resolution is not a direct one-to-one match (Figure 1b).

A 50-Watt LED flood light provided uniform illumination across the tank, while the Phantom Camera Control software facilitated synchronized operation of the imaging system. Gas flow regulation was achieved using a Dwyer Mass controller (0-500 mLPM), which enabled precise control over air injection rates. The system was connected to a pressurized air tank at one end, while the other end was linked to a 0.6 cm nozzle positioned at the tank's bottom center. The tank was filled with 29 cm of distilled water to simulate molten steel, with a 1.5 cm layer of aerated sunflower oil serving as a slag. This setup allowed controlled observations of bubble dynamics, interfacial disruptions, and the mechanisms of slag entrainment and inclusion transportation.

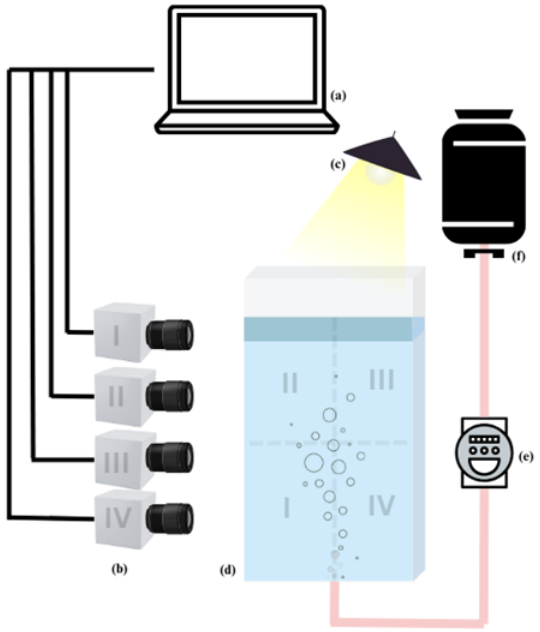

Figure 2: The experimental setup (a) Computer and image collecting system (b) High Speed Cameras (c) LED Lamp (d) Water ladle tank (e) flow rate meter/controller (f) Compressed air Tank

The experimental setup was developed in such a way that imitates slag entrainment conditions in an industrial steel ladle while keeping the variables under rigorous control to assure reproducibility. Before each experiment, the water tank was thoroughly cleaned to remove any remaining particles or oil, preventing any sort of contamination. Once cleaned, the tank was filled with distilled water and allowed to settle until all air bubbles were gone. Sunflower oil was chosen for its viscosity and dynamics similarity. To replicate the porous nature of slag from an actual industrial ladle, the sunflower oil was aerated for two minutes with an air compressor attached to a water filter. This method created air bubbles inside the oil, resulting foamy structures which resembled to actual metallurgical slag (Wang et al 2020).

The density and surface tension of the foamy oil was measured, as aeration of the sunflower oil affects both properties. Using the pendant drop method, the average surface tension of the foamy oil at room temperature was 27.62 mN/m, whereas untreated sunflower oil had the surface tension of 33.2 mN/m, indicating a 16.8% decrease due to aeration. The density of the foamy oil was 800 kg/m^3, and surface tension was calculated using the Open Drop software.

Multiple trials were taken to assure accuracy, and the findings confirmed that aeration considerably affected the oil's interfacial characteristics, allowing it to better simulate foamy slag in metallurgical operations. The foamy oil was then carefully placed over the distilled water surface on the tank to establish a homogenous layer before gas injection begins. Compressed air was supplied into the system through a nozzle at the bottom center on the tank with an initial flow of 150 milliliters per minute (mLPM). This injection of compressed air lasted for five minutes to simulate the real ladle conditions. During the experiment, every 20 seconds, the high-speed imaging system will record 40 millisecond long video (20 frames) on each camera under different flow rates ranging from 180 to 330 mLPM to investigate the influence of gas flow rate on slag entrainment. By systematically varying the flow rate, this study can reveal the correlation between gas injection flow rate and micro-entrainment for better understanding of the inclusion behavior in actual metallurgical process.

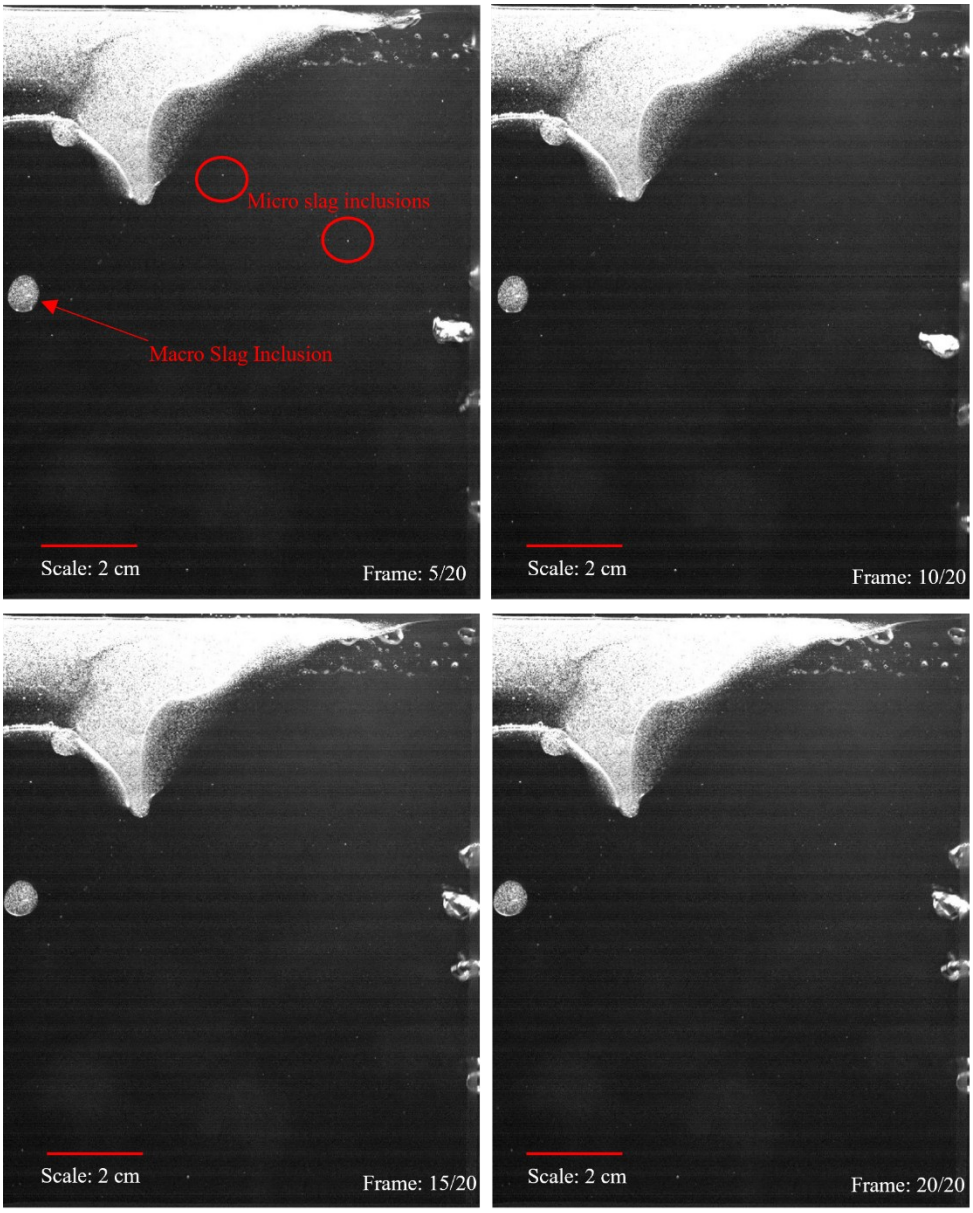

Figure 3: oil inclusions images at a gas injection rate of 240 mLPM

ImageJ, an open-source analytic program, was used to evaluate the experimental data and enable a thorough investigation of slag entrainment. For precise measurements, the pixels-to-micron scale had to be calibrated as the initial stage of picture processing. A physical ruler was inserted into the tank, and its pixel representation was measured in ImageJ to achieve calibration. To make sure for comparable readings across all quadrants, a distinct scale factor was assigned to each camera because their fields of vision varied slightly. After that, preprocessing techniques were used to improve the quality of the image. The first stage was to remove the background using the rolling radius techniques to fix uneven lighting. Static features were eliminated using the median image subtraction approach, which can be accessible using ImageJ's "Z Project" function, leaving only dynamic elements like inclusions, air bubbles.

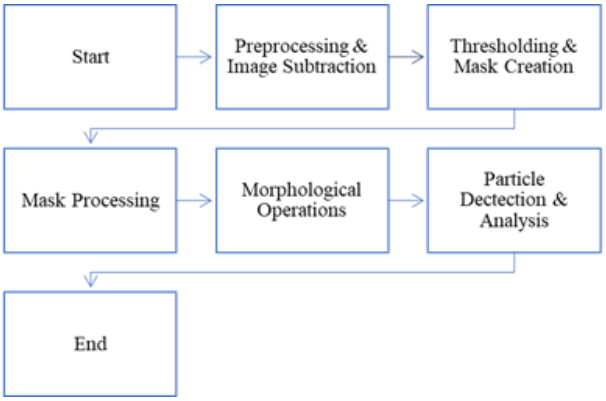

Figure 4: Image processing flow chart using ImageJ

Following preprocessing, thresholding and masking techniques were used to segment the image and extract the entrained oil and bubbles. Thresholding commonly employed intensity levels ranging from 25 to 30, with a maximum limit of 255. The "Intermodes" approach was used to build binary masks that increased the contrast between particles and backgrounds. Morphological methods such as median filtering and iterative dilation were used to improve particles detection by increasing visibility and decreasing noise. The "Fill Holes" tool was then used to close any gaps in the observed particles, resulting in complete segmentation. "Masking" is applied after the Fill Holes operation to exclude unwanted particles. Specifically, the slag particles which are still attached to slag layer, and as well as larger shed particles classifies as macro inclusions. This ensures that only relevant tiny particles are detected for the analysis. This step is particularly important at higher flow rates especially above 240 mLPM, where increased gas injection rate causes the shedding of larger macro particles. If these macro particles are not masked properly, they may be mistakenly counted as micro inclusion particles, affecting the accuracy of the results (See Figure 5).

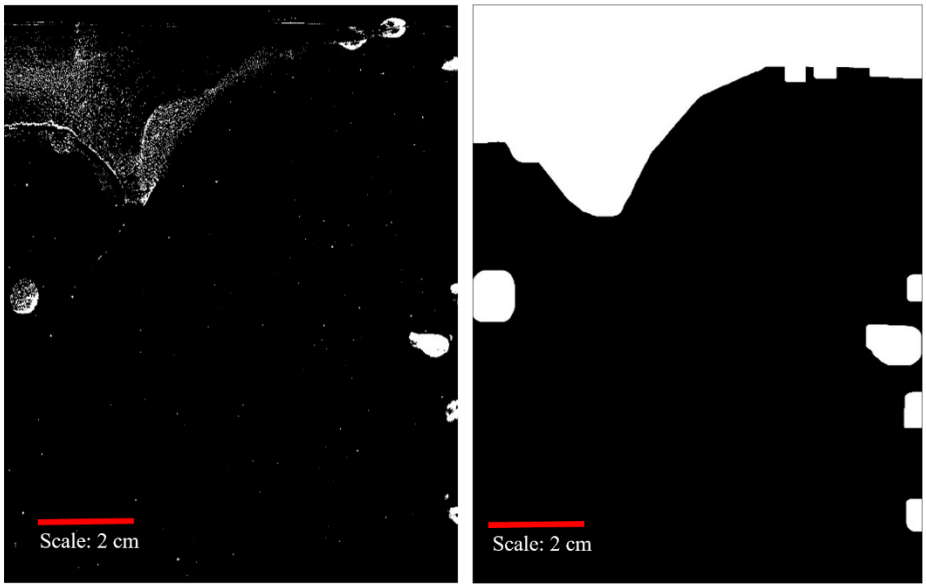

Figure 5: Example of image mask for targeting macro inclusion, air droplets and foamy oil.

Finally, the binary mask pictures were inverted and processed with ImageJ's "Image Multiplication" tool to detect entrained oil and bubbles. The "Analyze" module was then used to quantify particle count, size, and distribution at each flow rate and quadrant.

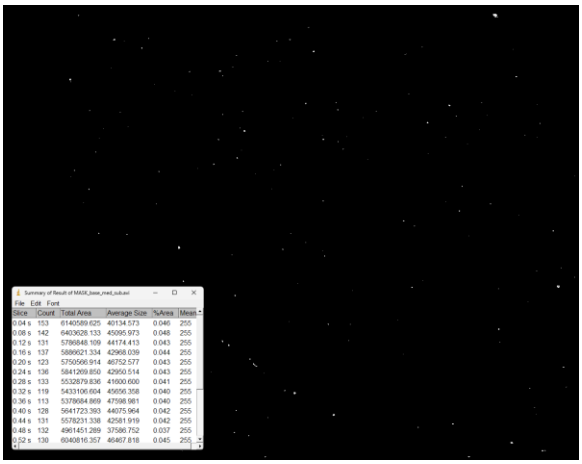

Figure 6: Particle detection and quantification

RESULTS

Once the particle count for each quadra is estimated from the ImageJ, the total particle count can be calculated and estimated from taking the sum of the particle count at any given time. Subsequently, the mean value of total particle count can be calculated over 40 milliseconds (20 frames) for every 20 seconds interval. Table 1 presents the results of the mean total particle count under different gas injection rates. Generally, higher gas injection rate will produce higher particle count and particle count increases over time once gas injection started. Figure 7 shows the plots of mean particle count at different gas injection rate versus time, revealing faster particle inclusion generation in the beginning and slower particle inclusion generation in later time. From 180 seconds after the gas injection starts, the change in particle count is becoming less significant, suggesting a stabilized particle/inclusion count value in the water ladle and equilibrium state of inclusion. Therefore, the averaged value of particle count is estimated between 180 seconds and 240 seconds to acquire the particle count of water ladle model at equilibrium state. The result is presented in table 2 and plotted in Figure 8. As expected, at equilibrium state of inclusion, the average particle count increases with gas injection rate. At low gas injection rate between 150 to 270 mLPM, the particle count increase rapidly from 471 to 940 while particle count reaches a relative stable value at around 1000 at higher gas injection rate above 270 mLPM.

Table 1: Particle count data over time under different gas injection rates

	Injection rate (mLPM)						
Time	**150**	**180**	**210**	**240**	**270**	**300**	**330**
5	36	128	45	72	48	92	104
20	140	187	120	177	165	324	260
40	303	278	201	328	317	425	458
60	363	332	269	416	426	543	577
80	366	386	439	507	462	606	625
100	396	496	518	664	599	718	744
120	435	523	524	729	667	759	816
140	443	555	586	727	757	835	918
160	482	539	621	770	860	887	967
180	469	544	679	782	886	933	978
200	463	558	666	802	910	974	982
220	463	547	696	811	947	1025	1081
240	464	555	702	801	921	1086	1086
260	492	581	721	822	960	1094	1085
280	481	570	738	813	969	1053	1098
300	480	565	698	833	980	1032	1051

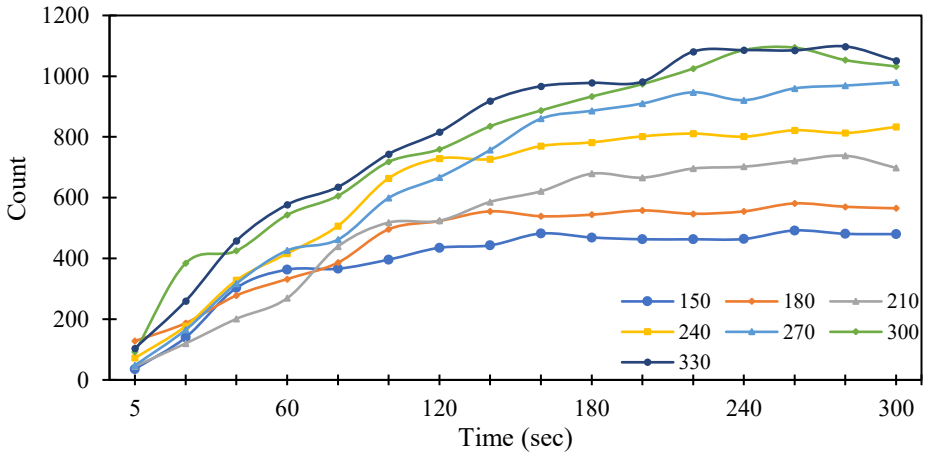

Figure 7: Particle count plot under different gas injection rates

Table 2: Aaverage particle count at equilibrium state

Gas injection rate (mLPM)	***Average Count***
150	471
180	561
210	703
240	808
270	940
300	1027
330	1057

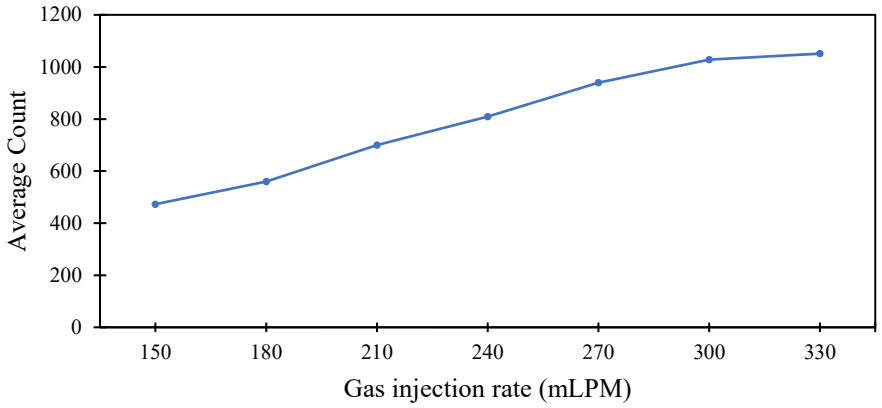

Figure 82: Average particle counts at equilibrium under different gas injection rates

CONCLUSION

In this study, a thin water ladle model is implemented to simulate slag entrainment with a focus of studying micro scale inclusion. Aerated sunflower seed oil is implemented to simulate the porous slag with distilled water to replicate the behavior of molten steel and controlled air injection. A high-speed/high-resolution photography system, consists of 4 cameras, is utilized to film the development of the flow and foamy oil, capturing macro- and micro-oil particle inclusions. Using ImageJ, quantification of entrained micro-oil particles is enabled. Particularly, images with micro particles can be extracted while large particle images are excluded from image masking. Therefore, micro inclusions during the experiments can be targeted and micro particle count can be quantified under different gas injection rates. The results clearly indicate a strong correlation between gas injection rate and micro particle entrainment. The particle count plots show steady increases in the beginning of gas injection, followed by stable particle count after 3 minutes of gas injection, suggesting an equilibrium state of inclusion. Consequently, particle count at equilibrium are evaluated under different gas injection rates. The result of particle count at equilibrium suggests a strong dependence on gas injection rate. At equilibrium, when gas injection rate is below 270 mLPM, particle counts increase with gas injection

rate, however, when the gas injection rate is above 270 mLPM, the particle count reaches a stable value at around 1000.

Therefore, gas injection rate is a key factor in controlling the micro inclusion behavior. At lower flow rates, entrainment was modest, with fewer particles crossing the water-oil interface. With higher flow rates significantly increasing the number of inclusions. As flow rates increased beyond 240 mLPM, entrainment became more aggressive, resulting in greater dispersion of slag into the water phase. This behavior was particularly visible in high frame rate images, as larger bubbles at higher flow rates, breaks up the foamy oil layer more effectively. Overall, the findings illustrated the importance of gas injection optimization in ladle metallurgy. By carefully managing flow rates, excessive slag entrainment may be reduced during ladle metallurgy.

ACKNOWLEDGEMENT

We would like to thank Armin Silean and Nicholas Walla for their valuable suggestions throughout the experiment. This work was supported in part by the National Science Foundation through its MRI program (CMMI-1919726) and GOALI program (CMMI-2113967). Support from all members of the Steel Manufacturing Simulation and Visualization Consortium (SMSVC), the SMSVC Ladle Project Technical Committee members, and Nucor Steel and the permission to publish this work are greatly acknowledged.

REFERENCES

1. April Pitts-Baggett, theoretical and experimental studies of dissimilar secondary metallurgy methods for improving steel cleanliness. Ph. D Thesis. 2017, The University of Alabama.
2. Diez, D., DeRose, J., & Locherer, T. (2020, April 28). *Rate the quality of your steel: Free Webinar and Report*. Science Lab | Leica Microsystems. https://www.leica-microsystems.com/science-lab/applied/rate-the-quality-of-your-steel-free-webinar-and-report/
3. Cao, J., Li, Y., Lin, W., Che, J., Zhou, F., Tan, Y., Li, D., Dang, J., & Chen, C. (2023). Assessment of inclusion removal ability in refining Slags containing CE2O3. Crystals, 13(2), 202. https://doi.org/10.3390/cryst13020202
4. Seetharaman, S., McLean, A., L., G. R. I., & Sridhar, S. (2014). *Treatise on Process Metallurgy Industrial Processes, Part A* (Vol. 3). Elsevier.
5. Costa e Silva, Non-metallic inclusion in steels origin and control. Journal of Material Research and Technology. Volume 7, Issue 3, 283-299.
6. Y. Miki and B.G. Thomas, Model of inclusion removal in a tundish. *Metallurgical and Materials Transactions B*, Volume 30, pages 639–654, in 1999.
7. Mona Akbari, Babak Safaei, Taleb Zarei, Investigation of gas purging configuration in an industrial ladle by computational fluid dynamics. *Physics of Fluid 35, 053334 (2023)*
8. R. Wang, B. Zhang, C. Liu, M. Jiang, Physical modeling of dynamic evolution of metallurgical slag foaming. Experimental Thermal and Fluid Science. 113 2020